Supporting Information for:

The influence of chemical composition, aerosol acidity, and metal dissolution on oxidative potential of fine particulate matter and redox potential of the lung lining fluid

Pourya Shahpoury,[1] Zheng Wei Zhang,[1] Andrea Arangio,[2] Valbona Celo,[3] Ewa Dabek-Zlotorzynska,[3] Tom Harner,[1] Athanasios Nenes[2,4]

[1]Air Quality Processes Research Section, Environment and Climate Change Canada, Toronto, Canada

[2]Laboratory of Atmospheric Processes and their Impacts, School of Architecture, Civil and Environmental Engineering, École Polytechnique Fédérale de Lausanne, Switzerland

[3]Analysis and Air Quality Section, Environment and Climate Change Canada, Ottawa, Canada

[4]Institute of Chemical Engineering Sciences, Foundation for Research and Technology Hellas, Patras, Greece

Correspondence: Pourya Shahpoury (pourya.shahpoury@canada.ca)

Contents

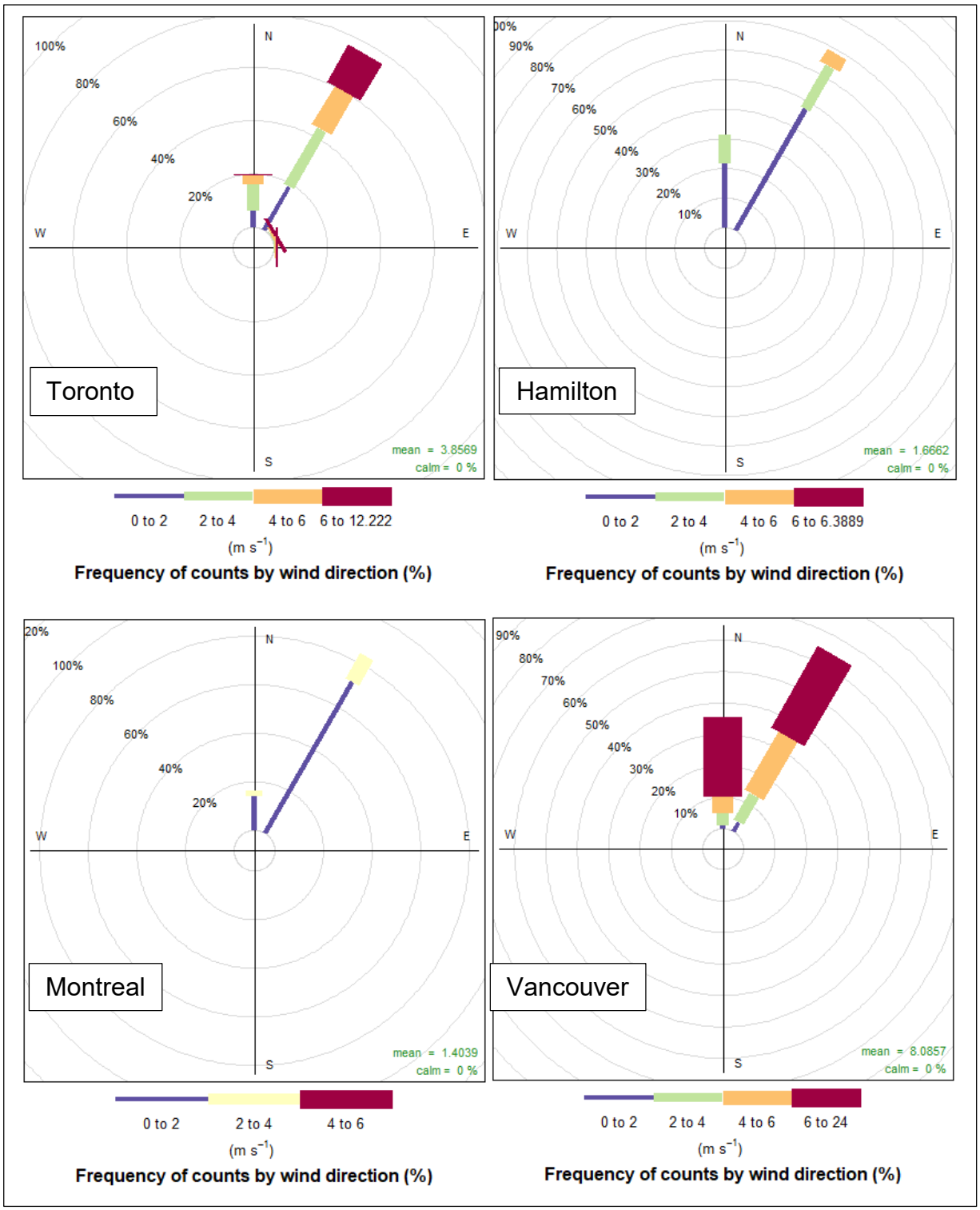

Figure S1. Wind roses obtained from hourly meteorological data for the sampling dates that were considered for oxidative potential analysis. The graphs show the percent frequency of counts by wind directions, as well as the color-coded wind speed across the study locations.

Section S1. Analysis and speciation of $PM_{2.5}$

The $PM_{2.5}$ samples collected on PTFE membranes were analyzed for 22 trace elements using nondestructive energy dispersive X–ray fluorescence spectrometry (ED-XRF, Epsilon 5, Malvern Panalytical Inc., Malvern, Montreal, QC, Canada). These included Al, Si, S, K, Ca, Ti, V, Cr, Mn, Fe, Ni, Zn, Se, Br, Rb, Sr, Cd, Sn, Sb, Cs, Ba, Pb. The $PM_{2.5}$ samples were also analyzed for 25 trace elements using inductively coupled plasma mass spectrometry (ICP-MS; Agilent Technologies, Wilmington, DE, USA). These trace elements were Cu, Fe, Mn, Be, Al, Ti, V, Cr, Co, Ni, Zn, As, Se, Sr, Mo, Ag, Cd, Sn, Sb, Ba, La, Ce, Tl, Pb, U. The water-soluble cations and anions were analyzed using ion chromatography (IC, Thermo Scientific, Sunnyvale, CA, USA). The species included fluoride, acetate, formate, propionate, methanesulfonic acid, chloride, nitrite, sulphate, oxalate, bromide, nitrate, phosphate, lithium, sodium, ammonium, potassium, magnesium, calcium, strontium, barium. In addition, acidic and basic gaseous species were also analyzed with IC. These species were NH_3, HNO_3, HONO, and SO_2.

Table S1. Calculation method used for reconstruction of $PM_{2.5}$ mass [a]

$PM_{2.5}$ component	Abbreviation	Mass calculation
Black carbon	BC	[EC]
Organic Matter	OM [b]	[OC]×1.6
Ammonium sulfates: $(NH_4)_2SO_4$, $(NH_4)_3H(SO_4)_2$, NH_4HSO_4	$(NH_4)_2SO_4$ [c]	$[SO_4^{2-}] + [NH_4^+] - 0.29 \times [NO_3^-]$
Ammonium nitrate	NH_4NO_3	$1.29 \times [NO_3^-]$
Sodium chloride	NaCl	[Na] + [Cl]
Mineral dust	MD	3.48 × [Si] + 1.63 × [Ca] + 2.42 × [Fe] + 1.41 × [K] + 1.94 × [Ti]
Trace element oxides	TEO	1.47 × [V] + 1.29 × [Mn] + 1.27 × [Ni] + 1.25 × [Cu] + 1.24 × [Zn] + 1.32 × [As] + 1.08 × [Pb] + 1.2 × [Se] + 1.37 × [Sr] + 1.31 × [Cr]
Unidentified [d]	UI	$[PM_{2.5}] - ([BC] + [OM] + [(NH_4)_2SO_4] + [NH_4NO_3] + [NaCl] + [MD] + [TEO])$

[a] Adopted from Dabek-Zlotorzynska et al., (2019); [b] we used the correction factor of 1.6 recommended for converting OC to OM for urban particulate matter (Turpin and Lim, 2001); [c] $(NH_4)_2SO_4$ represents all ammonium sulfate species and is used here for simplicity; [d] represents the aerosol mass that could not be identify, corresponding to $PM_{2.5}$ water content, chemical species that were not targeted for analysis, and uncertainty related to estimation of OM.

Section S2. Estimation of aerosol pH

The aerosol pH was calculated using ISORROPIA II model (Fountoukis and Nenes, 2007). The model performs thermodynamic equilibrium calculation for an inorganic aerosol system, with input parameters consisting of aerosol precursors NH_3, Na, Ca, K, Mg, HNO_3, HCl, and H_2SO_4, as well as ambient temperature and relative humidity. The inclusion of the crustal material Ca, K, and Mg in this model improves the prediction of ammonium and nitrate partitioning in the aerosol and the estimation of pH, particularly when crustal dust constitutes a considerable fraction of $PM_{2.5}$. ISORROPIA II determines a set of sub-system equilibrium equations and solves the equations for equilibrium state using the chemical potential method (Fountoukis and Nenes, 2007). The modelled aerosol system consists of potential components in the gas-phase, i.e. NH_3, HNO_3, HCl, H_2O, in the liquid-phase, i.e. NH_4, Na^+, H^+, Cl^-, NO_3^-, SO_4^{2-}, HNO_3, NH_3, HCl, HSO_4^-, OH^-, H_2O, Ca^{2+}, K^+, Mg^{2+}, and in the solid phase, i.e. $(NH_4)_2SO_4$, NH_4HSO_4, $(NH_4)_3H(SO_4)_2$, NH_4NO_3, NH_4Cl, NaCl, $NaNO_3$, $NaHSO_4$, Na_2SO_4, $CaSO_4$, $Ca(NO_3)_2$, $CaCl_2$, K_2SO_4, $KHSO_4$, KNO_3, KCl, $MgSO_4$, $Mg(NO_3)_2$, and $MgCl_2$. For HNO_3, where measured values were not available, mean of available values were used for pH calculations. The model output is the concentration of H^+ which is converted to pH using the aerosol liquid water content (LWC). Further details about the pH calculation method and the treatment of input parameters can be found in (Fountoukis and Nenes, 2007).

Table S2a. Concentrations of chemical species in $PM_{2.5}$ from near-road sites

	Toronto		Vancouver	
	Min-Max	**Mean ± SD (Median)**	**Min-Max**	**Mean ± SD (Median)**
$PM_{2.5}$ **(μg m^{-3})** [a]	10-30.4	17.3±6.2 (15.3)	1.1-27	8.9±4.8 (8.3)
BC [a]	0.7-2.9	2±0.8 (2.2)	0.5-2.8	1.5±0.7 (1.3)
OC [a]	0.8-4.2	2.6±1 (2.6)	0.7-10	2.3±1.9 (2)
$(NH_4)_2SO_4$ [a]	1-5.3	2.2±1.2 (1.8)	0.1-2.4	0.7±0.6 (0.5)
NH_4NO_3 [a]	0.04-14.4	2.6±4.2 (0.2)	0.09-3.1	0.6±0.7 (0.4)
NaCl [a]	0.09-0.64	0.17±0.2 (0.09)	0.09-1.38	0.23±0.34 (0.09)
MD [a]	0.3-2.5	1.3±0.7 (1.1)	0.22-1.09	0.52±0.24 (0.44)
TEO [a]	0-0.21	0.08±0.05 (0.07)	0-0.07	0.03±0.02 (0.03)
UI [a]	1.5-6.7	3.8±1.5 (3.7)	0.4-5.2	2.4±1.4 (2.2)
∑TMs (WS) [a]	0.04-0.22	0.12±0.06 (0.11)	0.01-0.08	0.03±0.02 (0.02)
∑TMs (WI) [a]	0.06-0.57	0.25±0.16 (0.2)	0.06-0.29	0.13±0.06 (0.1)
∑TMs (NT) [a]	0-0.68	0.34±0.21 (0.32)	0-0.34	0.15±0.08 (0.13)
$C_2O_4^{2-}$ [a]	0.04-0.26	0.13±0.07 (0.12)	0.01-0.43	0.06±0.09 (0.03)
Levoglucosan **(ng m^{-3})** [b]	12.5-263.2	64.3±70.3 (26.6)	6.6-402.4	160.3±113.9 (138.7)
Mannosan [b]	1.4-36.2	8.3±10 (4.1)	2.1-115.6	39.7±30.5 (31.7)
Galactosan [b]	1.9-12.3	4.8±3.8 (3.8)	2.5-27.9	11.9±7.7 (8.9)
∑Monosaccharides [b]	12.5-311.6	73.5±83.2 (28.5)	6.6-545.9	204.9±152.4 (162.8)
Arabitol [b]	0.6-4.8	2.6±1.5 (2.5)	0.7-4.8	1.9±1.2 (1.5)
Mannitol [b]	2.7-4.1	3.6±0.5 (3.7)	1.7-7.6	2.9±1.5 (2.4)
∑Polyols [b]	0.6-8.6	4.2±3.0 (4.1)	0.7-12.0	4.5±2.7 (3.5)
Cu (NT) [b]	2.5-25.0	11.8±6.8 (11.8)	0.5-18.8	8.5±3.9 (8.4)
Fe (NT) [b]	47.1-589.0	260.6±157 (204.6)	1.7-275.6	119.7±64.2 (107.5)
Mn (NT) [b]	1.6-15.0	5±3.3 (4.3)	0-4.9	2±1.3 (1.7)
Ti (NT) [b]	0.6-14.2	6±4 (4.4)	0.1-8.4	3.6±1.9 (3.1)
V (NT) [b]	0.07-0.73	0.28±0.14 (0.23)	0-1.96	0.58±0.52 (0.48)
Cr (NT) [b]	0.3-2.3	1±0.5 (0.9)	0.1-1.26	0.59±0.34 (0.49)
Co (NT) [b]	0.01-0.08	0.04±0.02 (0.03)	0-0.05	0.02±0.01 (0.02)
Ni (NT) [b]	0.08-0.88	0.44±0.2 (0.43)	0.07-1.6	0.52±0.35 (0.42)
Zn (NT) [b]	8.6-154.1	40.8±37.7 (25.6)	0.7-24.8	9.7±5.8 (8)
Mo (NT) [b]	0.20-1.05	0.5±0.22 (0.5)	0-0.82	0.4±0.19 (0.36)
Ag (NT) [b]	0.06-0.12	0.07±0.01 (0.06)	0.012-0.1	0.02±0.018 (0.012)
Cd (NT) [b]	0.05-0.28	0.12±0.06 (0.09)	0.01-0.19	0.05±0.04 (0.04)
Cu (WS) [b]	1.4-17.2	8±4 (7.7)	1.1-9	4±1.8 (3.5)
Fe (WS) [b]	8.8-132.6	62.1±37.1 (57.6)	1.7-58	11.4±11 (8.7)
Mn (WS) [b]	1-8	3±1.4 (3.3)	0.2-5.8	1.2±1.2 (0.9)
Ti (WS) [b]	0.14-5.09	0.99±0.98 (0.76)	0.06-1.11	0.21±0.21 (0.17)
V (WS) [b]	0.04-0.53	0.19±0.12 (0.15)	0.03-1.13	0.33±0.28 (0.24)
Cr (WS) [b]	0.08-0.73	0.39±0.15 (0.4)	0.1-7.79	0.45±1.53 (0.1)
Co (WS) [b]	0.005-0.032	0.019±0.007 (0.021)	0.002-0.023	0.009±0.007 (0.008)
Ni (WS) [b]	0.1-0.4	0.19±0.08 (0.17)	0.05-0.66	0.19±0.16 (0.14)
Zn (WS) [b]	8.5-123.8	39.2±31.2 (26.2)	2.2-20.4	8.4±4.5 (7.7)
Mo (WS) [b]	0.13-0.62	0.33±0.14 (0.28)	0.05-0.58	0.22±0.12 (0.2)
Ag (WS) [b]	0.009-0.043	0.012±0.008 (0.009)	0.002-0.011	0.003±0.002 (0.002)
Cd (WS) [b]	0.05-0.27	0.12±0.06 (0.1)	0.02-0.16	0.05±0.04 (0.03)

[a] concentration unit is μg m^{-3}; [b] the unit is ng m^{-3}; BC: black carbon; OC: organic carbon; MD: mineral dust; TEO: trace element oxides; UI: unidentified; TMs: transition metals; WS: water-soluble; WI: water-insoluble; NT: near-total; ∑Monosaccharides: sum of the concentrations of levoglucosan, mannosan, and galactosan; ∑Polyols: sum of the concentrations of arabitol and mannitol.

Table S2b. Concentrations of chemical species in $PM_{2.5}$

	Hamilton		Montreal	
	Min-Max	**Mean ± SD (Median)**	**Min-Max**	**Mean ± SD (Median)**
$PM_{2.5}$ **(μg m^{-3})** [a]	13.5-26.8	16.8±3.3 (15.3)	13.4-28.5	17.6±4.6 (15.6)
BC [a]	0-2.4	1.2±0.5 (1.2)	0.1-2.8	1.2±0.6 (1.1)
OC [a]	1.2-4.5	2.8±0.9 (2.7)	0.7-7.8	3.9±1.5 (3.6)
$(NH_4)_2SO_4$ [a]	1-10.8	3.5±2.3 (2.9)	0-3	1.7±0.9 (1.7)
NH_4NO_3 [a]	0.1-11.5	3.4±3.3 (2.3)	0.1-8.8	3.3±3 (3.6)
NaCl [a]	0.04-0.31	0.11±0.07 (0.09)	0.19-0.83	0.44±0.23 (0.42)
MD [a]	0.06-1.78	0.7±0.47 (0.55)	0.14-1.97	0.90±0.66 (0.66)
TEO [a]	0-0.27	0.07±0.06 (0.05)	0.01-0.11	0.06±0.03 (0.07)
UI [a]	1-5.9	3.8±1.4 (3.8)	1.2-4.0	2.6±1.2 (2.7)
∑TMs (WS) [a]	0-0.22	0.09±0.06 (0.07)	0.01-0.1	0.05±0.03 (0.04)
∑TMs (WI) [a]	0-0.36	0.08±0.09 (0.05)	0.01-0.2	0.08±0.06 (0.06)
∑TMs (NT) [a]	0.01-0.59	0.16±0.14 (0.10)	0.01-0.28	0.13±0.09 (0.11)
$C_2O_4^{2-}$ [a]	0.01-0.28	0.13±0.08 (0.14)	0.01-0.27	0.13±0.1 (0.1)
Levoglucosan **(ng m^{-3})** [b]	6.4-405.2	89.4±96.7 (59)	11.1-1313.9	331.9±346.3 (252.9)
Mannosan [b]	2.5-52.8	15.2±14.1 (10.8)	0.7-169.6	41.1±40.6 (36.4)
Galactosan [b]	0.6-23.3	6.2±5.5 (5.6)	0.4-57.4	16.6±14.9 (13.9)
∑Monosaccharides [b]	6.4-481.3	101.9±114.2 (68.9)	11.1-1540.9	382.9±400.2 (303.9)
Arabitol [b]	1-6.1	2.7±1.4 (2.4)	1.2-7.3	3.6±1.9 (3.2)
Mannitol [b]	3.2-8.3	4.9±1.9 (4)	0.7-7.5	3.6±2.4 (3.2)
∑Polyols [b]	1.0-14.4	4.4±3.7 (3.4)	1.2-14.7	5.7±4.2 (4.3)
Cu (NT) [b]	0.4-16.7	5.5±3.8 (4.6)	0.7-15.5	5±4.1 (4.6)
Fe (NT) [b]	10-387	110.1±93.7 (73.3)	8.4-209.6	84.9±63.1 (67.1)
Mn (NT) [b]	0.3-35.9	7.4±8.8 (3)	0.2-7.4	3.5±2.5 (2.8)
Ti (NT) [b]	0.4-5.9	1.6±1.5 (1.2)	0.4-10.8	4±3.3 (3.6)
V (NT) [b]	0.04-1.58	0.46±0.36 (0.43)	0.01-0.82	0.36±0.24 (0.36)
Cr (NT) [b]	0.11-2	0.58±0.41 (0.44)	0.26-1.17	0.6±0.37 (0.54)
Co (NT) [b]	0-0.07	0.03±0.02 (0.02)	0-0.13	0.04±0.04 (0.03)
Ni (NT) [b]	0.66-1.22	0.68±0.1 (0.66)	0.21-0.86	0.47±0.29 (0.34)
Zn (NT) [b]	1-147.2	34.3±36.5 (19.7)	3.1-46.4	25.7±16.2 (22.1)
Mo (NT) [b]	0.02-1.08	0.38±0.27 (0.32)	0.01-1.64	0.41±0.45 (0.32)
Ag (NT) [b]	0.04-0.12	0.04±0.01 (0.04)	0.01-1.04	0.14±0.32 (0.04)
Cd (NT) [b]	0.01-0.43	0.14±0.09 (0.12)	0.02-0.43	0.23±0.15 (0.29)
Cu (WS) [b]	0.5-21.2	4.9±4.5 (3.6)	0.3-11.8	3.4±2.6 (2.9)
Fe (WS) [b]	0.9-106.5	38.5±28.6 (26.8)	1-61.8	26.9±16.1 (25.1)
Mn (WS) [b]	0.1-26.1	6.3±6.7 (2.7)	0.2-6.7	2.9±1.7 (2.6)
Ti (WS) [b]	0.1-1.28	0.43±0.28 (0.4)	0.1-5.5	1.3±1.6 (0.5)
V (WS) [b]	0-1.37	0.39±0.33 (0.34)	0-1.66	0.47±0.43 (0.27)
Cr (WS) [b]	0.15-0.58	0.3±0.13 (0.28)	0.15-0.49	0.3±0.11 (0.28)
Co (WS) [b]	0.002-0.057	0.018±0.011 (0.016)	0.003-0.063	0.025±0.016 (0.019)
Ni (WS) [b]	0.06-0.66	0.21±0.15 (0.21)	0.08-0.46	0.26±0.11 (0.26)
Zn (WS) [b]	2.3-124.4	35.1±33.9 (21.7)	5.6-41.4	21±10.8 (20.6)
Mo (WS) [b]	0.04-1.02	0.31±0.22 (0.26)	0.18-1.4	0.37±0.3 (0.3)
Ag (WS) [b]	0.002-0.023	0.007±0.006 (0.006)	0.002-0.168	0.03±0.046 (0.01)
Cd (WS) [b]	0.01-0.49	0.15±0.11 (0.12)	0.03-0.38	0.18±0.09 (0.17)

[a] concentration unit is μg m^{-3}; [b] the unit is ng m^{-3}; BC: black carbon; OC: organic carbon; MD: mineral dust; TEO: trace element oxides; UI: unidentified; TMs: transition metals; WS: water-soluble; WI: water-insoluble; NT: near-total; ∑Monosaccharides: sum of the concentrations of levoglucosan, mannosan, and galactosan; ∑Polyols: sum of the concentrations of arabitol and mannitol.

Section S3. Composition of $PM_{2.5}$ across the study locations

Figure S2a-b shows the concentrations of major $PM_{2.5}$ species reconstructed using formulas in Table S1. Toronto had the highest levels of BC (median: 2.2 μg m^{-3}; Figure S2a, Table S2a-b), whereas Vancouver, Hamilton, and Montreal demonstrated relatively low but similar values (median: 1.1-1.3 μg m^{-3}). The relatively high BC levels at Toronto site are explained by the intense traffic in the vicinity of the sampling site (3 m away; daily average of ~412000 vehicles in 2016; this includes diesel emission from passing trucks). The highest and lowest median values for OM were found in Montreal and Vancouver (5.8 and 3.2 μg m^{-3}, respectively), while Toronto and Hamilton showed median values in between this range (4.2 and 4.3 μg m^{-3}; Figure S2a). The levels of $(NH_4)_2SO_4$ were noticeably higher in Hamilton (median: 2.9, and the upper bound of 10.8 μg m^{-3}), compared to the other sites (median: 0.5-1.8, and the upper bound of ≤5.3 μg m^{-3}); this observation is in line with the industrial activities surrounding this study location. In addition, Hamilton and Montreal had the highest levels of NH_4NO_3 among other sites (median: 2.3 and 3.6 μg m^{-3}) compared to the other two sites, i.e. 0.2-0.4 μg m^{-3}. $(NH_4)_2SO_4$ and NH_4NO_3 are produced in the atmosphere following the reaction of NH_3 with H_2SO_4 and HNO_3, respectively (Seigneur, 2019). The reaction of NH_3 with the former is favored under typical atmospheric conditions, leading to the formation of $(NH_4)_2SO_4$. However, urban areas with high NH_3 emission and photo-chemically formed HNO_3 could create local conditions that are thermodynamically favorable to formation of NH_4NO_3 (Nowak et al., 2010). This pattern was observed with the Montreal study site. This site also demonstrated the highest levels of NaCl (median: 0.4 μg m^{-3}; Figure 1a), which may indicate contribution from road salts applied during the winter months (Montreal typically receives the highest amount of snow annually among the study locations).

The highest levels of mineral dust were observed in Toronto (median: 1.1 μg m^{-3}), while the other locations showed similar median values (0.4-0.7 μg m^{-3}). High levels of mineral dust in Toronto are due to the near-road nature of this site and the traffic-related resuspension of the road dust that contributes to the $PM_{2.5}$ mass (Dabek-Zlotorzynska et al., 2019). Toronto and Montreal had the highest values of trace element oxides (0.07 μg m^{-3}), followed by Hamilton and Vancouver (0.05 and 0.03 μg m^{-3}, respectively).

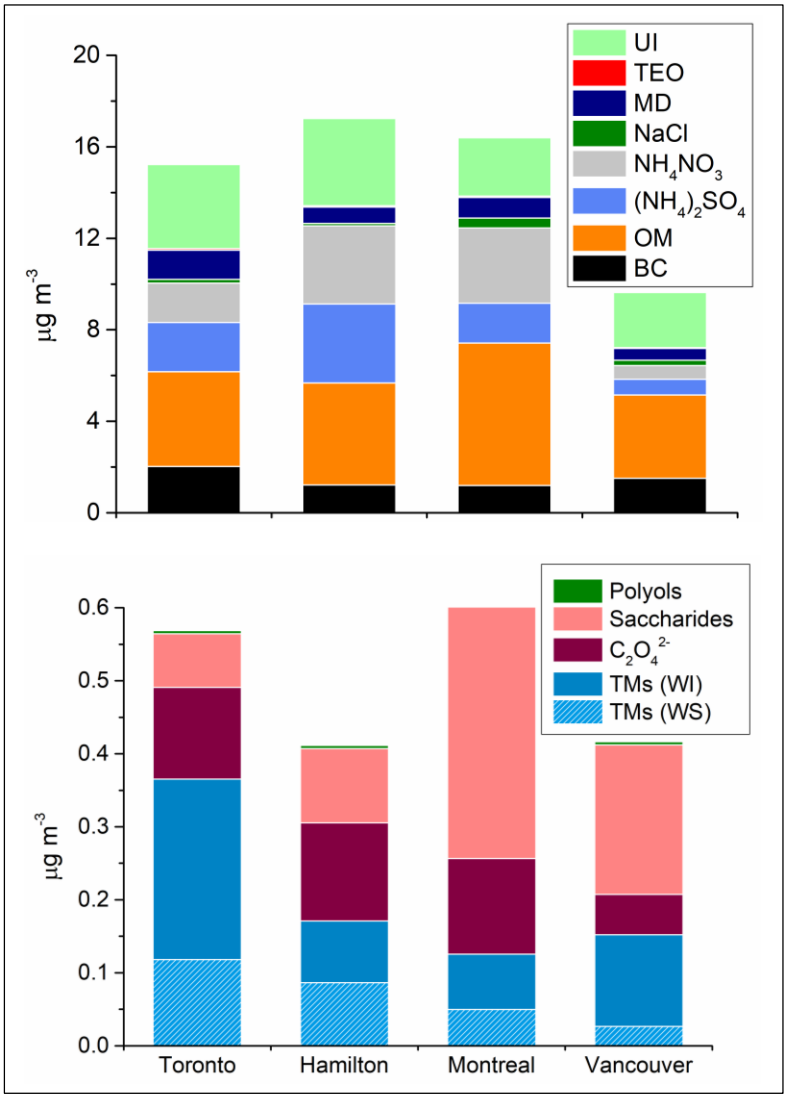

Figure S2. $PM_{2.5}$ compositions across the study locations; BC: black carbon, OM: organic matter, MD: mineral dust (i.e. Si, Ca, Fe, K, Ti), TEO: trace element oxides (i.e. V, Mn, Ni, Cu, Zn, As, Pb, Se, Sr, Cr), UI: unidentified chemicals, TMs: transition metals, WS: water-soluble, WI: water-insoluble, saccharides (i.e. monosaccharide anhydrides/biomass burning tracers: levoglucosan, mannosan, galactosan), and polyols (biogenic emission tracers: arabitol and mannitol). For simplicity, $(NH_4)_2SO_4$ represents all ammonium sulfate species considered in mass reconstruction, including $(NH_4)_3H(SO_4)_2$ and NH_4HSO_4.

Table S3. $PM_{2.5}$ chemical species (μg m^{-3}), ambient temperature (°C) and relative humidity (%) used for pH estimation

	Toronto		Vancouver	
	Min-Max	**Mean ± SD (Median)**	**Min-Max**	**Mean ± SD (Median)**
$NH_{3(g)}$	0.5-11.1	5.6±2.9 (5.6)	2.6-6.7	4.2±1.4 (3.8)
$HNO_{3(g)}$	0.3-1.5	0.9±0.5 (0.8)	0.07-1.05	0.21±0.3 (0.07)
$NH_4^+{}_{(aq)}$	0.3-3.4	1.1±1 (0.6)	0.08-1.03	0.26±0.27 (0.16)
$Na^+{}_{(aq)}$	0.02-0.3	0.08±0.09 (0.04)	0.02-0.66	0.15±0.18 (0.07)
$Ca^{2+}{}_{(aq)}$	0.02-0.67	0.16±0.16 (0.13)	0.02-0.15	0.04±0.03 (0.03)
$K^+{}_{(aq)}$	0.02-0.12	0.06±0.03 (0.05)	0.02-0.15	0.05±0.04 (0.03)
$Mg^+{}_{(aq)}$	0.01-0.04	0.02±0.01 (0.03)	0.005-0.04	0.012±0.011 (0.005)
$Cl^-{}_{(aq)}$	0.05-0.39	0.10±0.12 (0.05)	0.05-0.84	0.14±0.21 (0.05)
$NO_3^-{}_{(aq)}$	0-11.2	2.0±3.3 (0.1)	0.07-2.4	0.46±0.54 (0.3)
$SO_4^{2-}{}_{(aq)}$	0.8-4.1	1.7±0.9 (1.4)	0.17-1.7	0.57±0.4 (0.42)
T (°C)	-11.4-25.9	12.9±12.1 (18.8)	-2.3-19.4	9.5±6.2 (10.5)
RH (%)	50-87	67±11 (66)	56-96	82±10 (84)
LWC	0.4-22.4	5.1±6.5 (2.6)	0.8-29.2	5.1±7.8 (2.1)
pH	1.6-5.1	3.2±1.0 (3.0)	2.4-7.4	3.8±1.1 (3.5)
	Hamilton		**Montreal**	
$NH_{3(g)}$	0.5-11.6	4±2.1 (4.1)	0.5-6	2.4±1.5 (2.8)
$HNO_{3(g)}$	0.4-1.2	0.6±0.3 (0.4)	0.3-0.7	0.6±0.1 (0.6)
$NH_4^+{}_{(aq)}$	0.2-3	1.3±0.8 (1.1)	0.01-2.11	1.04±0.6 (0.89)
$Na^+{}_{(aq)}$	0.02-0.10	0.03±0.02 (0.02)	0.02-0.39	0.09±0.12 (0.02)
$Ca^{2+}{}_{(aq)}$	0.02-0.23	0.1±0.06 (0.09)	0.02-0.34	0.13±0.12 (0.09)
$K^+{}_{(aq)}$	0.01-0.14	0.05±0.03 (0.05)	0.02-0.23	0.09±0.05 (0.09)
$Mg^+{}_{(aq)}$	0-0.06	0.02±0.01 (0.02)	0.003-0.026	0.013±0.008 (0.011)
$Cl^-{}_{(aq)}$	0.02-0.19	0.06±0.04 (0.05)	0.02-0.50	0.15±0.15 (0.05)
$NO_3^-{}_{(aq)}$	0-8.9	1.7±2.4 (0.6)	0-6.8	2.5±2.4 (2.8)
$SO_4^{2-}{}_{(aq)}$	0.8-8.1	2.6±1.7 (2.3)	0-2.3	1.4±0.6 (1.4)
T (°C)	-2.1-26.5	14.5±9 (16.1)	-11.4-26.5	9.4±13.1 (13.1)
RH (%)	45-100	74±14 (77)	34-95	68±16 (71)
LWC	0.5-46.1	9.0±9.9 (5.0)	0.7-44.3	8.0±13.9 (2.8)
pH	1.8-3.7	2.7±0.6 (2.8)	1.8-4.2	2.9±1.0 (2.9)

n = 14 at Toronto (only covering samples from 2017), 20 at Vancouver, 26 at Hamilton, and 9 at Montreal. pH was only calculated for those samples for which all required speciation data were available. LWC: aerosol liquid water content (μg m^{-3}) estimated with ISORROPIA model.

Table S4a. Results of principal component and multiple linear regression analysis in Toronto

Toronto	**Factor 1**		**Factor 2**		**Factor 3**		**Factor 4**	
% Variance	27		17		17		16	
% $PM_{2.5}$ mass - Cold	-		-		48		17	
% $PM_{2.5}$ mass – Warm	17		-		60		-	
Factor loading (factor score coefficient)	Fe	0.88 (0.23)	Si	0.88 (0.44)	Oxa	0.94 (0.43)	NO_3	0.92 (0.39)
	Cu	0.88 (0.27)	Al	0.86 (0.40)	OC	0.82 (0.33)	NH_4	0.86 (0.30)
	Sn	0.87 (0.28)	Ca	0.79 (0.33)	SO_4	0.71 (0.26)	Lev	0.74 (0.29)
	EC	0.78 (0.22)						
	Mn	0.75 (0.14)						
	Zn	0.62 (0.15)						
Potential sources	Brake wear/tailpipe emission		Crustal matter		Aged combustion aerosols		Biomass burning	

The values in brackets are the factor score coefficients for individual species

Table S4b. Results of principal component and multiple linear regression analysis in Vancouver

Vancouver	**Factor 1**		**Factor 2**		**Factor 3**		**Factor 4**	
% Variance	37		15		14		14	
% $PM_{2.5}$ mass – Cold	54		-		-		-	
% $PM_{2.5}$ mass – Warm	-		40		23		-	
Factor loading (factor score coefficient)	Fe	0.95 (0.21)	Lev	0.88 (0.41)	NH4	0.90 (0.44)	Si	0.86 (0.51)
	Mn	0.89 (0.21)	NO3	0.71 (0.28)	SO4	0.90 (0.40)	Al	0.61 (0.23)
	Cu	0.88 (0.16)	K	0.69 (0.39)	Oxa	0.63 (0.22)		
	Sn	0.87 (0.17)						
	Zn	0.86 (0.19)						
	EC	0.84 (0.13)						
	OC	0.64 (0.03)						
Potential sources	Brake wear/tailpipe emission		Biomass burning		Aged combustion aerosols		Crustal matter	

Table S4c. Results of principal component and multiple linear regression analysis in Hamilton

Hamilton	**Factor 1**		**Factor 2**		**Factor 3**		**Factor 4**	
% Variance	30		20		15		15	
% $PM_{2.5}$ mass – Cold	-		48		26		-	
% $PM_{2.5}$ mass – Warm	-		92		-		-	
Factor loading (factor score coefficient)	Mn	0.87 (0.26)	Oxa	0.91 (0.44)	NO3	0.91 (0.42)	Si	0.83 (0.52)
	Fe	0.84 (0.23)	OC	0.88 (0.40)	NH4	0.90 (0.38)	Ca	0.72 (0.37)
	Zn	0.83 (0.27)	EC	0.71 (0.25)	Lev	0.71 (0.26)	Al	0.69 (0.37)
	Pb	0.82 (0.24)						
	Sn	0.79 (0.20)						
	Cu	0.65 (0.16)						
Potential sources	Industrial-metallurgical emissions/brake wear		Aged combustion aerosols		Biomass burning		Crustal matter	

Table S4d. Results of principal component and multiple linear regression analysis in Montreal

Montreal	**Factor 1**		**Factor 2**		**Factor 3**	
% Variance	35		23		18	
% $PM_{2.5}$ mass – Cold	11		9		55	
% $PM_{2.5}$ mass – Warm	-		-		66	
Factor loading (factor score coefficient)	Fe	0.90 (0.20)	NO3	0.91 (0.32)	Oxa	0.84 (0.45)
	Al	0.90 (0.20)	Lev	0.86 (0.30)	SO4	0.82 (0.41)
	Mn	0.83 (0.20)	NH4	0.74 (0.18)	OC	0.65 (0.24)
	Si	0.83 (0.18)	K	0.64 (0.17)		
	Ca	0.80 (0.19)				
	Cu	0.73 (0.13)				
Potential sources	Crustal material		biomass burning		Aged combustion aerosols	

Figure S3. Distribution (%) of water-soluble and water-insoluble transition metals in $PM_{2.5}$ across study locations. The graphs depict the median concentrations.

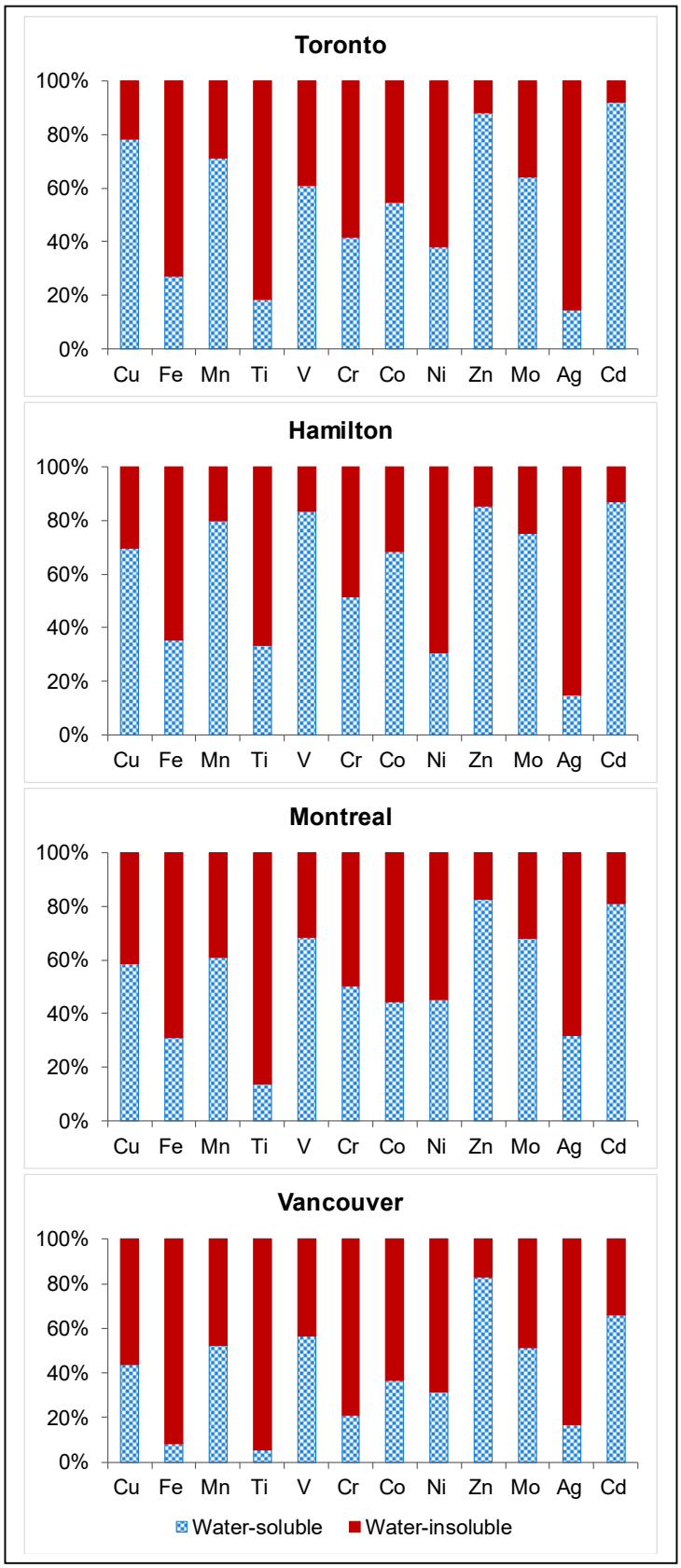

Figure S4. Heatmaps of Spearman correlation between oxidative potential indicators across the sites. Correlations are shown as coefficients × 100 and as color-coded ellipses. The latter can be seen as the visual illustration of scatterplots, with high positive correlations appearing as narrow ellipses at 45 degrees and in dark red, and low correlations appearing as ovals in orange.

Table S5. OP indicators measured across the study sites

	Toronto		Vancouver	
	Min-Max	**Mean ± SD (Median)**	**Min-Max**	**Mean ± SD (Median)**
AA (nmol min^{-1} m^{-3})	57-676	310±200 (240)	53-317	174±93 (144)
GSH (nmol min^{-1} m^{-3})	111-880	499±232 (535)	84-313	194±67 (183)
GSSG (nmol min^{-1} m^{-3})	72-363	202±85 (190)	57-176	112±32 (116)
CSH (nmol min^{-1} m^{-3})	101-821	471±225 (529)	78-330	195±69 (185)
CSSC (nmol min^{-1} m^{-3})	9-150	71±44 (71)	14-65	38±14 (38)
$Eh_{GSH\text{-}GSSG}$ (mV)	18-108	52±28 (47)	17-45	29±7 (25)
$Eh_{CSH\text{-}CSSC}$ (mV)	20-144	67±37 (64)	22-56	40±9 (38)
RP (mV)	6-87	38±24 (33)	n/a	n/a
	Hamilton		**Montreal**	
AA (nmol min^{-1} m^{-3})	47-591	256±153 (257)	20-503	183±149 (144)
GSH (nmol min^{-1} m^{-3})	40-469	223±130 (174)	43-388	193±104 (213)
GSSG (nmol min^{-1} m^{-3})	25-256	123±58 (101)	37-182	113±41 (116)
CSH (nmol min^{-1} m^{-3})	41-505	234±143 (174)	35-390	206±100 (215)
CSSC (nmol min^{-1} m^{-3})	17-119	46±27 (31)	5-43	22±13 (19)
$Eh_{GSH\text{-}GSSG}$ (mV)	8-69	32±16 (25)	10-34	22±8 (21)
$Eh_{CSH\text{-}CSSC}$ (mV)	23-87	46±18 (36)	13-49	31±12 (29)
RP (mV)	4-51	20±14 (14)	3-32	15±8 (13)

AA: ascorbic acid; GSH: glutathione; GSSG: glutathione disulfide; CSH: cysteine; CSSC: cystine; Eh: estimated redox potential of SELF based on GSH/GSSG and CSH/CSSC redox pairs; RP: redox potential of SELF measured using the oxidation-reduction sensor.

Figure S5a. Seasonal variation of oxidative potential across the study sites, $Eh_{GSH\text{-}GSSG}$ (mV). There was no statistically significant difference in Eh between the warm and cold periods at each site (Mann–Whitney test; $p > 0.05$).

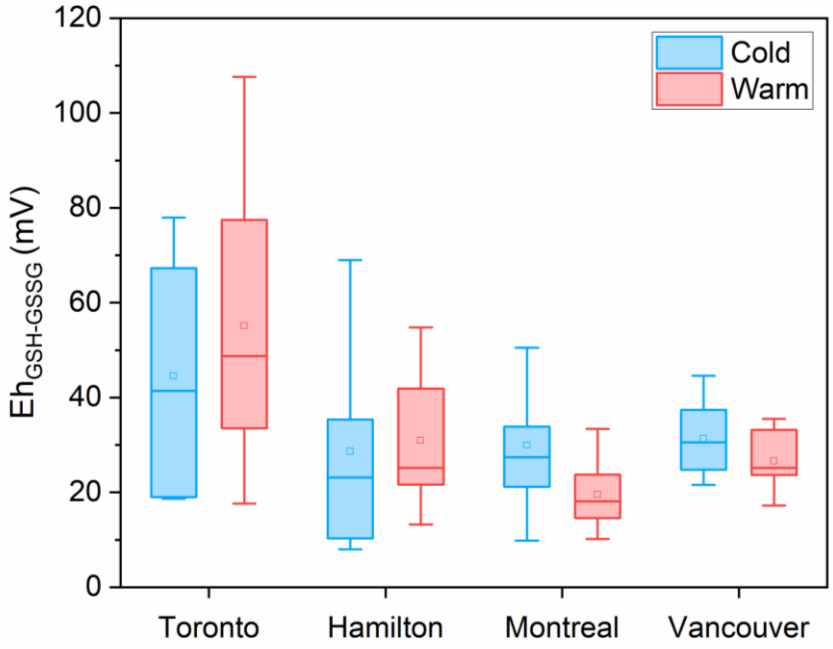

Figure S5b. Seasonal variation of oxidative potential across the study sites, OP_{AA} (nM min^{-1} m^{-3}). Vancouver data was not included since there was only one value that fell in the warm period. There was no statistically significant difference in Eh between the warm and cold periods at each site (Mann–Whitney test; $p > 0.05$).

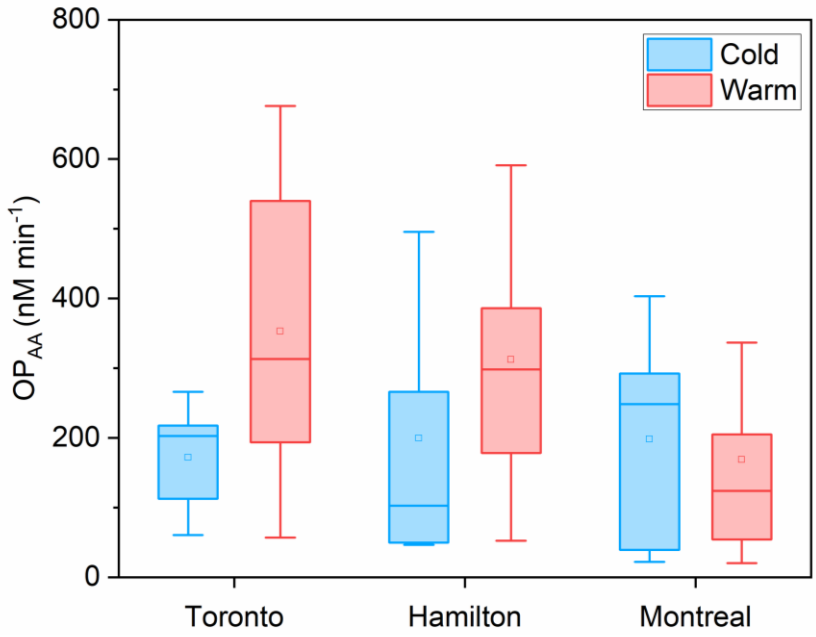

Figure S6. Heatmaps of Spearman correlation between OP indicators and total and water-soluble $PM_{2.5}$ species from combined samples.

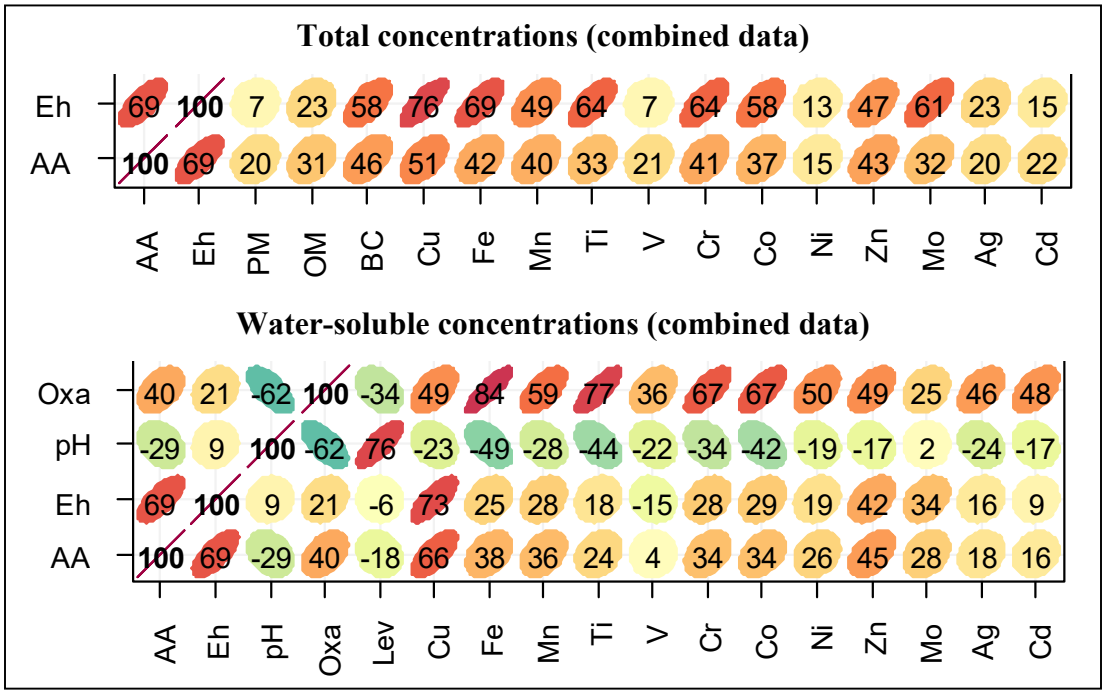

Figure S7. Heatmaps of Spearman correlation between pH, $PM_{2.5}$ composition, temperature, and relative humidity.

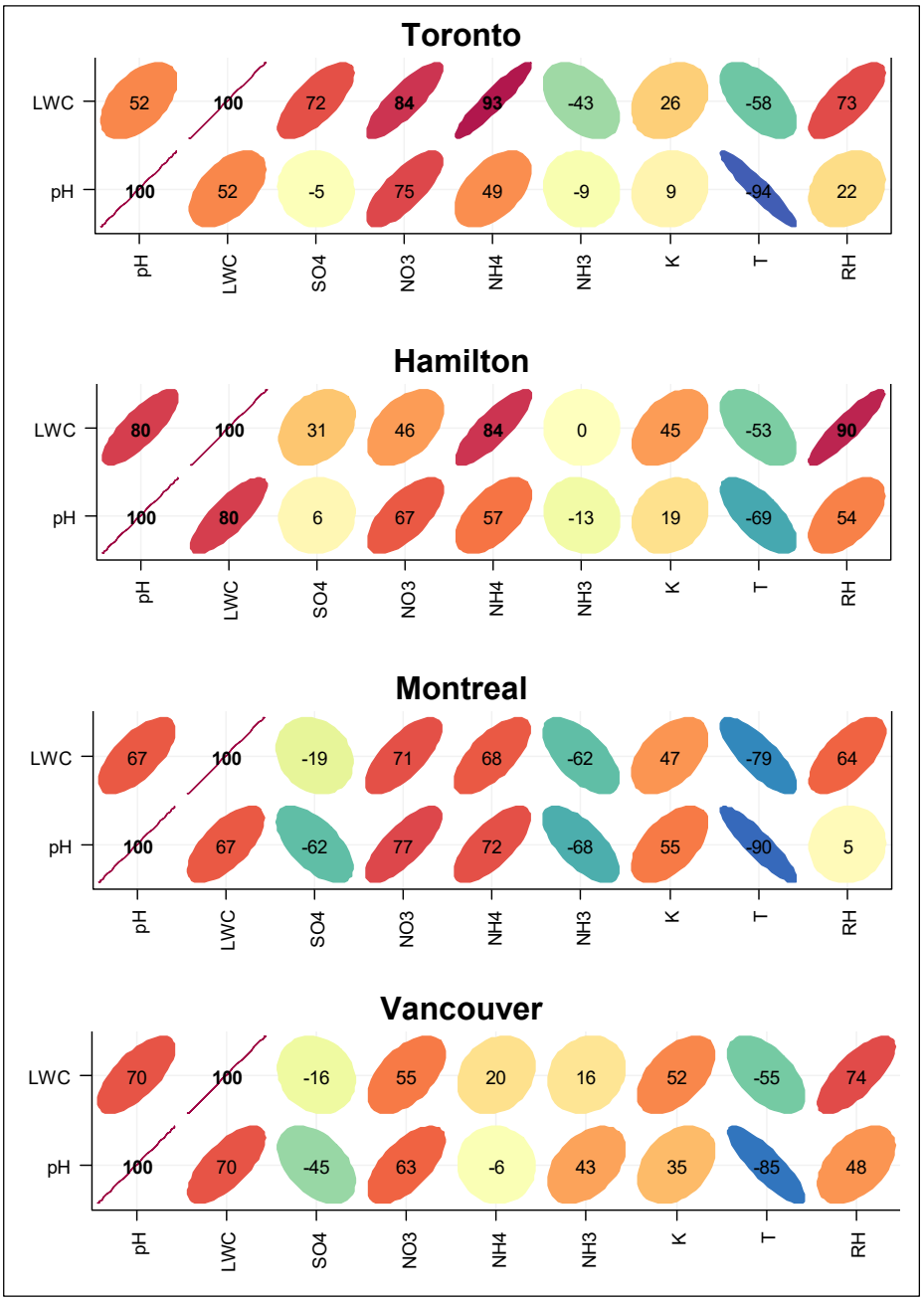

LWC: aerosol liquid water content estimated with ISORROPIA model. pH was only estimated for 2017 samples for Toronto and Montreal, due to the lack of PM speciation data from 2016. Correlations are shown as coefficients × 100 and as color-coded ellipses (high positive correlation in dark red and high negative correlation in dark blue).

References

Dabek-Zlotorzynska, E., Celo, V., Ding, L., Herod, D., Jeong, C. H., Evans, G. and Hilker, N.: Characteristics and sources of PM2.5 and reactive gases near roadways in two metropolitan areas in Canada, Atmos. Environ., 218, 116980, 2019.

Fountoukis, C. and Nenes, A.: ISORROPIA II: a computationally efficient thermodynamic equilibrium model for $K^+ - Ca^{2+} - Mg^{2+} - NH_4^+ - Na^+ - SO_4^{2-} - NO_3^-$, $-Cl^- - H_2O$, Atmos. Chem. Phys., 7, 4639–4659, 2007.

Nowak, J. B., Neuman, J. A., Bahreini, R., Brock, C. A., Middlebrook, A. M., Wollny, A. G., Holloway, J. S., Peischl, J., Ryerson, T. B. and Fehsenfeld, F. C.: Airborne observations of ammonia and ammonium nitrate formation over Houston, Texas, J. Geophys. Res., 115, 22304, doi:10.1029/2010JD014195, 2010.

Seigneur, C.: Air Pollution, Cambridge University Press, Cambridge., pp. 190-236, 2019.

Turpin, B. J. and Lim, H. J.: Species contributions to PM2.5 mass concentrations: Revisiting common assumptions for estimating organic mass, Aerosol Sci. Technol., 35, 602–610, 2001.